

Suppression of hysteresis in a forced van der Pol–Duffing oscillator

Abdelhak Fahsi^b, Mohamed Belhaq^{a,*}, Faouzi Lakrad^a

^a University Hassan II-Aïn Chock, Casablanca, Morocco

^b University Hassan II-Mohammadia, FSTM, Mohammadia, Morocco

ARTICLE INFO

Article history:

Received 15 March 2008

Received in revised form 17 March 2008

Accepted 17 March 2008

Available online 25 March 2008

PACS:

02.30.Hq

02.30.Oz

02.30.Mv

46.40.Ff

Keywords:

Hysteresis suppression

Frequency locking

High-frequency excitation

Perturbation analysis

ABSTRACT

This paper examines the suppression of hysteresis in a forced nonlinear self-sustained oscillator near the fundamental resonance. The suppression is studied by applying a rapid forcing on the oscillator. Analytical treatment based on perturbation analysis is performed to capture the entrainment zone, the quasiperiodic modulation domain and the hysteresis area as well. The analysis leads to a strategy for the suppression of hysteresis occurring between 1:1 frequency-locked motion and quasiperiodic response. This hysteresis suppression causes the disappearance of nonlinear effects leading to a smooth transition between the quasiperiodic and the frequency-locked responses. Specifically, it appears that a rapid forcing introduces additional apparent nonlinear stiffness which can effectively suppress hysteresis in a certain range of the rapid excitation frequency. This work was motivated by the important issue of controlling and eliminating hysteresis often undesirable in mechanical systems, in general, and in application to microscale devices, especially.

© 2008 Elsevier B.V. All rights reserved.

1. Introduction

This work investigates the effect of adding a fast harmonic excitation (FHE) on a hysteresis loop occurring in a frequency-locked area. The presence of hysteresis in this area produces changes in the response between quasiperiodic (QP) behavior and frequency-locked oscillation. This undesirable effect was reported and analyzed in optically driven MEMS resonators; see [1] and references therein. In microbeam-based resonator hysteresis phenomenon has also been addressed; see [2] and references therein. It was shown in [2] that the attenuation of hysteresis can be achieved by acting on the quality factor which is related to the damping. Therefore, the suppression of hysteresis is of great importance to avoid abrupt changes in the dynamic and to insure a smooth transition between stable responses.

The purpose of this paper is to examine the hysteresis suppression by introducing a FHE to the considered system. We consider a canonical model exhibiting hysteresis effect and QP response and we use perturbation analysis to generate analytical expression predicting the values range of the fast excitation for which the hysteresis is completely eliminated.

Early works [3–5] have used the idea of adding FHE to study the well-known effect of stabilization of an inverted pendulum on a vibrating support. Other effects of FHE have been addressed, such as equilibrium stability [6], linear stiffness [7], natural frequencies [8], resonant behavior [9], symmetry breaking [10], and limit cycles [11,12].

The canonical model that captures the essential nonlinear phenomena to be examined is a forced van der Pol–Duffing oscillator subjected to a FHE in the dimensionless form

$$\ddot{x} + x - (\alpha - \beta x^2)\dot{x} - \gamma x^3 = h \cos \omega t + a\Omega^2 \cos x \cos \Omega t, \quad (1)$$

* Corresponding author.

E-mail address: mbelhaq@yahoo.fr (M. Belhaq).

where damping α , β , nonlinearity γ and excitation amplitudes h and a are small. We assume that the FHE frequency Ω is large compared to the frequency of the external forcing ω such that the resonance between the two frequencies is avoided. In recent works [13,14], a van der Pol–Mathieu–Duffing oscillator was investigated. It was shown in [14] that FHE can change the nonlinear characteristic behavior of the oscillator from softening to hardening. Here, we focus attention on the suppression of entrained hysteresis in Eq. (1) near the fundamental resonance 1:1.

In the following sections, we use the method of direct partition of motion (DPM) to derive an equation governing the slow dynamic of the oscillator (1). Next, we perform the multiple scales method on the slow dynamic near the resonance 1:1 to obtain a slow flow of the slow dynamic. Analysis of equilibria of this slow flow provides the amplitude–frequency response and the entrainment area. A multiple scales method is performed in a second step on the slow flow to obtain analytical expressions of QP solutions and their modulation domain. Analytical prediction of the variation of the hysteresis area as function of the frequency Ω is provided. We perform numerical calculations and we compare to analytical results for validation.

2. Slow dynamic and entrainment

We examine the effect of a FHE on the slow dynamic of system (1) by using the method of DPM [15]. We introduce two different time scales $T_0 = \Omega t$ (fast time) and $T_1 = t$ (slow time) and we split up $x(t)$ into a slow part $z(T_1)$ and a fast part $\epsilon\phi(T_0, T_1)$ as follows:

$$x(t) = z(T_1) + \epsilon\phi(T_0, T_1), \quad (2)$$

where z describes slow main motions at time scale of oscillations, $\epsilon\phi$ stands for an overlay of the fast motions and ϵ indicates that $\epsilon\phi$ is small compared to z . The fast part $\epsilon\phi$ and its derivatives are assumed to be 2π -periodic functions of fast time T_0 with zero mean value with respect to this time, so that $\langle x(t) \rangle = z(T_1)$ where $\langle \cdot \rangle \equiv \frac{1}{2\pi} \int_0^{2\pi} (\cdot) dT_0$ defines time-averaging operator over one period of the fast excitation with the slow time T_1 fixed. Since Ω is considered to be large, we choose $\epsilon \equiv \Omega^{-1}$, for convenience.

Introducing $D_1^j \equiv \frac{\partial^j}{\partial T_1^j}$ yields $\frac{d}{dt} = \Omega D_0 + D_1$, $\frac{d^2}{dt^2} = \Omega^2 D_0^2 + 2\Omega D_0 D_1 + D_1^2$ and substituting (2) into (1) gives

$$\begin{aligned} \epsilon^{-1} D_0^2 \phi + 2D_0 D_1 \phi + \epsilon D_1^2 \phi + D_1^2 z + z + \epsilon\phi - (\alpha - \beta(z + \epsilon\phi)^2)(D_0 \phi + \epsilon D_1 \phi + D_1 z) - \gamma(z + \epsilon\phi)^3 \\ = h \cos \omega T_1 + \epsilon^{-1} (a\Omega) \cos(z + \epsilon\phi) \cos T_0. \end{aligned} \quad (3)$$

Averaging (3) leads to

$$D_1^2 z + z - (\alpha - \beta z^2) D_1 z - \gamma z^3 = h \cos \omega T_1 + \epsilon^{-1} (a\Omega) \langle \cos(z + \epsilon\phi) \cos T_0 \rangle. \quad (4)$$

Subtracting (4) from (3) yields

$$\begin{aligned} \epsilon^{-1} D_0^2 \phi + 2D_0 D_1 \phi + \epsilon D_1^2 \phi + \epsilon\phi - (\alpha - \beta z^2)(D_0 \phi + \epsilon D_1 \phi) + \beta(2\epsilon\phi + \epsilon^2 \phi^2)(D_0 \phi + \epsilon D_1 \phi) - \gamma(3\epsilon z^2 \phi + 3\epsilon^2 z \phi^2 + \epsilon^3 \phi^3) \\ = \epsilon^{-1} (a\Omega) \cos(z + \epsilon\phi) \cos T_0 - \epsilon^{-1} (a\Omega) \langle \cos(z + \epsilon\phi) \cos T_0 \rangle \end{aligned} \quad (5)$$

An approximate expression for $\epsilon\phi$ is obtained from (5) by considering only the terms of order ϵ^{-1} as

$$D_0^2 \phi = (a\Omega) \cos z \cos T_0. \quad (6)$$

The quantity $a\Omega$ represents the intensity of the excitation and it is assumed to be of the order of unity, $a\Omega = O(1)$. The stationary solution to the first order for ϕ is written as

$$\epsilon\phi = -a \cos z \cos T_0. \quad (7)$$

The equation governing the slow motion is derived from (4). Inserting $\cos(z + \epsilon\phi) = \cos z - \epsilon\phi \sin z + O(\epsilon^2)$ into Eq. (4) and retaining the dominant terms of order ϵ^0 , we obtain

$$D_1^2 z + z - (\alpha - \beta z^2) D_1 z - \gamma z^3 = h \cos \omega T_1 - (a\Omega) \sin z \langle \phi \cos T_0 \rangle. \quad (8)$$

Inserting ϕ from (7) and using that $\langle \cos^2 T_0 \rangle = 1/2$ we find the approximate equation for slow motions

$$D_1^2 z + z - (\alpha - \beta z^2) D_1 z - \gamma z^3 = h \cos \omega T_1 + \frac{1}{2} (a\Omega)^2 \cos z \sin z. \quad (9)$$

We analyze small vibrations around the origin by expanding in Taylor's series the terms $\sin z \simeq z - z^3/6$ and $\cos z \simeq 1 - z^2/2$. Keeping only terms up to order three in z , Eq. (9) becomes

$$D_1^2 z + \left(1 - \frac{1}{2} (a\Omega)^2\right) z - (\alpha - \beta z^2) D_1 z - \left(\gamma - \frac{1}{3} (a\Omega)^2\right) z^3 = h \cos \omega T_1. \quad (10)$$

In Eq. (10) of the slow dynamic, it appears that the effect of a FHE introduces additional apparent stiffness in the linear stiffness [6] and in the nonlinear one. These effects have been observed in a spring-connected two-link mechanism at a vibrating support [9].

Hence, Eq. (10) can be written as

$$\ddot{z} + \omega_0^2 z = (\alpha - \beta z^2)\dot{z} + \xi z^3 + h \cos \omega t, \tag{11}$$

where $\omega_0^2 = 1 - \frac{1}{2}(a\Omega)^2$ and $\xi = \gamma - \frac{1}{3}(a\Omega)^2$.

To investigate the dynamic near the fundamental resonance, we introduce a detuning parameter σ and we express the resonant condition by

$$\omega_0^2 = \omega^2 + \sigma. \tag{12}$$

A complete analytical analysis on periodic and QP responses requires the application of a double perturbation technique by introducing two small bookkeeping parameters μ and η . To derive a slow flow, we use the parameter μ in the first perturbation and we introduce the other parameter η in a second step for implementing the second perturbation on the slow flow. This procedure of using a perturbation analysis on a slow flow in systems under QP excitation has been proposed in [16] and applied to obtain analytical expressions of QP solutions [17] and of the stability chart for QP Mathieu equations [18–20]. Hence, at the first step Eq. (11) reads

$$\ddot{z} + \omega^2 z = \mu\{-\sigma z + (\alpha - \beta z^2)\dot{z} + \xi z^3 + h \cos \omega t\}. \tag{13}$$

Using the multiple scales technique [21], we seek a solution to Eq. (13) in the form

$$z(t) = z_0(T_1, T_2) + \mu z_1(T_1, T_2) + O(\mu^2), \tag{14}$$

where $T_1 = t$ and $T_2 = \mu t$. In terms of the variables T_i , the time derivatives become $\frac{d}{dt} = D_1 + \mu D_2 + O(\mu^2)$ and $\frac{d^2}{dt^2} = D_1^2 + 2\mu D_1 D_2 + O(\mu^2)$ where $D_i^j = \frac{\partial^j}{\partial T_i^j}$. Substituting (14) into (13), equating coefficients of like powers of μ , removing secular terms and using the expressions $\frac{d}{dt} = \mu D_2 + O(\mu^2)$ and $\frac{d^2}{dt^2} = \mu D_2^2 + O(\mu^2)$, we obtain a solution to the first order

$$z_0(T_1, T_2) = r(T_2) \cos(\omega T_1 + \theta(T_2)), \tag{15}$$

where the slow flow modulation equations of amplitude and phase are given by

$$\begin{aligned} \frac{dr}{dt} &= \frac{\alpha}{2} r - \frac{\beta}{8} r^3 - \frac{h}{2\omega} \sin(\theta), \\ r \frac{d\theta}{dt} &= \frac{\sigma}{2\omega} r - \frac{3\xi}{8\omega} r^3 - \frac{h}{2\omega} \cos(\theta). \end{aligned} \tag{16}$$

Equilibria of the slow flow (16), corresponding to periodic oscillations in the slow dynamic equation (11), are determined by setting $\frac{dr}{dt} = \frac{d\theta}{dt} = 0$. Using the relation $\cos^2 \theta + \sin^2 \theta = 1$ and assuming $\rho = r^2$, we obtain the following cubic equation in ρ :

$$A\rho^3 + B\rho^2 + C\rho + D = 0, \tag{17}$$

where $A = \frac{\beta^2}{64} + \frac{9\xi^2}{64\omega^2}$, $B = -(\frac{\alpha\beta}{8} + \frac{3\sigma\xi}{8\omega^2})$, $C = \frac{\alpha^2}{4} + \frac{\sigma^2}{4\omega^2}$ and $D = -\frac{h^2}{4\omega^2}$. The discriminant of Eq. (17) reads

$$\Delta = \frac{P^3}{27} + \frac{Q^2}{4}, \tag{18}$$

where $P = \frac{C}{A} - \frac{B^2}{3A^2}$ and $Q = \frac{2}{27}(\frac{B}{A})^3 - \frac{BC}{3A^2} + \frac{D}{A}$. Eq. (17) has three real positive roots if Δ is negative. Furthermore, Eq. (17) has only one positive root if Δ is positive. In what follows, we choose the parameters $\alpha = 0.01$, $\beta = 0.05$, $\gamma = 0.1$, $h = 0.1$ and $a = 0.02$.

In Fig. 1a the amplitude-frequency response curve, as given by Eq. (17), is presented for $\Omega = 0$. The solid lines denote stable branches and the dashed lines denote unstable ones. The effect of Ω on the frequency response curve is illustrated in Figs. 1b and c for the values $\Omega = 25$ and $\Omega = 40$. As in [14], it can be seen that as Ω increases, the backbone curve shifts right and its nonlinear characteristic moves from softening to hardening. For validation, analytical approximations are compared to numerical integration (circles) using a Runge–Kutta method.

3. Hysteresis suppression and quasiperiodic modulation

We transform the polar form (16) using the variable change $u = r \cos \theta$, $v = -r \sin \theta$ and we perform a second perturbation analysis by introducing the parameter η in damping and nonlinearity. We obtain the Cartesian system

$$\begin{aligned} \frac{du}{dt} &= \frac{\sigma}{2\omega} v + \eta \left\{ \frac{\alpha}{2} u - \left(\frac{\beta}{8} u + \frac{3\xi}{8\omega} v \right) (u^2 + v^2) \right\}, \\ \frac{dv}{dt} &= -\frac{\sigma}{2\omega} u + \frac{h}{2\omega} + \eta \left\{ \frac{\alpha}{2} v - \left(\frac{\beta}{8} v - \frac{3\xi}{8\omega} u \right) (u^2 + v^2) \right\}. \end{aligned} \tag{19}$$

Approximation of periodic solutions of the slow flow (19), corresponding to quasiperiodic responses in the slow dynamic (11), can be obtained by applying a multiple scales technique [16,18] on the system (19). We expand solutions as

$$\begin{aligned} u(t) &= u_0(T_1, T_2) + \eta u_1(T_1, T_2) + O(\eta^2), \\ v(t) &= v_0(T_1, T_2) + \eta v_1(T_1, T_2) + O(\eta^2), \end{aligned} \tag{20}$$

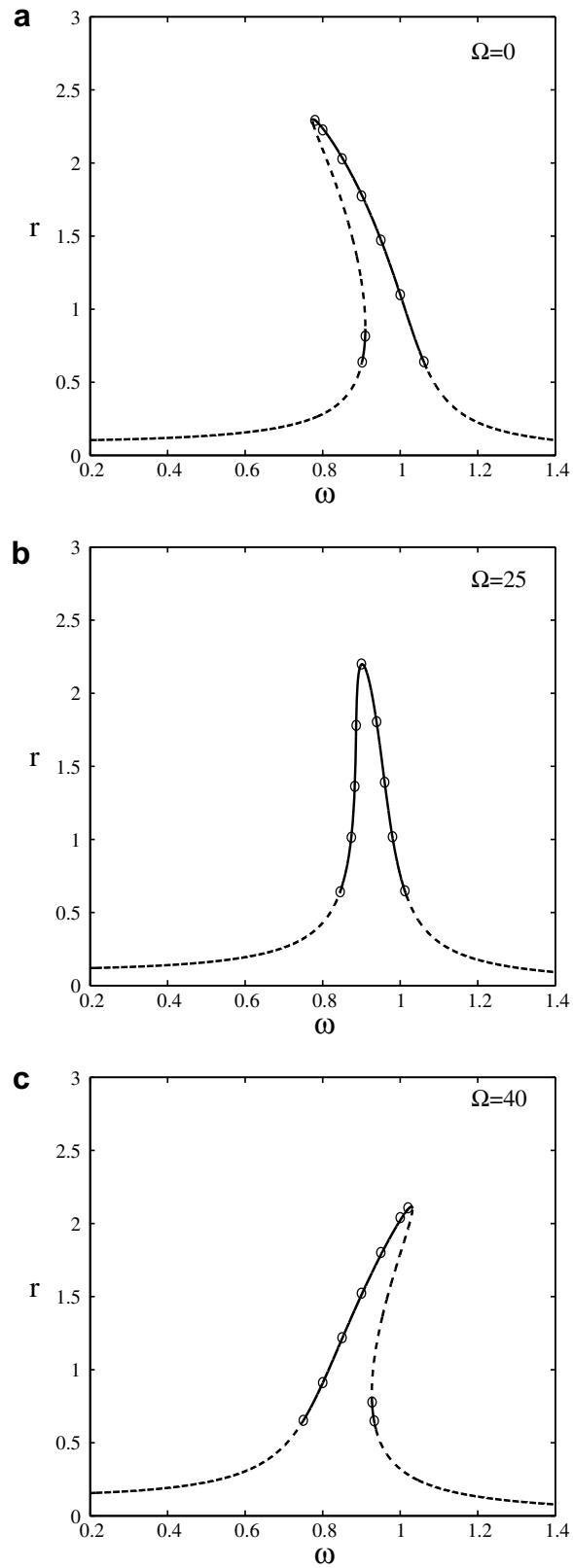


Fig. 1. Amplitude–frequency response for different values of the frequency ω . Analytical approximation: Solid (for stable) and dashed (for unstable). Numerical simulation: circles.

where $T_1 = t$ and $T_2 = \eta t$. Introducing $D_i = \frac{\partial}{\partial T_i}$ yields $\frac{d}{dt} = D_1 + \eta D_2 + O(\eta^2)$, substituting (20) into (19) and collecting terms, we obtain

- Order η^0 :

$$\begin{aligned} D_1^2 u_0 + v^2 u_0 &= \frac{\sigma}{2\omega} \frac{h}{2\omega}, \\ \frac{\sigma}{2\omega} v_0 &= D_1 u_0. \end{aligned} \tag{21}$$

- Order η^1 :

$$\begin{aligned} D_1^2 u_1 + v^2 u_1 &= \frac{\sigma}{2\omega} \left[-D_2 v_0 + \frac{\alpha}{2} v_0 - \left(\frac{\beta}{8} v_0 - \frac{3\xi}{8\omega} u_0 \right) (u_0^2 + v_0^2) \right] \\ &\quad - D_1 D_2 u_0 + \frac{\alpha}{2} D_1 u_0 - D_1 \left[\left(\frac{\beta}{8} u_0 + \frac{3\xi}{8\omega} v_0 \right) (u_0^2 + v_0^2) \right], \\ \frac{\sigma}{2\omega} v_1 &= D_1 u_1 + D_2 u_0 - \frac{\alpha}{2} u_0 + \left(\frac{\beta}{8} u_0 + \frac{3\xi}{8\omega} v_0 \right) (u_0^2 + v_0^2). \end{aligned} \tag{22}$$

where $\frac{v}{2\omega}$ is the natural frequency of system (19) corresponding to the frequency of the slow flow limit cycle.

The solution to the first order system (21) is given by

$$\begin{aligned} u_0(T_1, T_2) &= \frac{h}{\sigma} + R(T_2) \cos(vT_1 + \varphi(T_2)), \\ v_0(T_1, T_2) &= -\frac{2\omega}{\sigma} vR(T_2) \sin(vT_1 + \varphi(T_2)). \end{aligned} \tag{23}$$

Substituting (23) into (22) and removing secular terms, we obtain the following slow flow system on R and φ :

$$\begin{aligned} \frac{dR}{dt} &= \left(\frac{\alpha}{2} - \frac{\beta h^2}{4\sigma^2} \right) R - \frac{\beta}{8} R^3, \\ \frac{d\varphi}{dt} &= -\frac{3\xi\sigma}{8\omega|\sigma|} R^2 - \frac{3\xi h^2}{4\omega\sigma|\sigma|}. \end{aligned} \tag{24}$$

Thus, an approximate periodic solution of the slow flow (19) is given by

$$\begin{aligned} u(t) &= \frac{h}{\sigma} + R \cos(vt + \varphi), \\ v(t) &= -\frac{2\omega}{\sigma} vR \sin(vt + \varphi), \end{aligned} \tag{25}$$

and an approximate QP response of the slow dynamic (11) reads

$$z(t) = u(t) \cos(\omega t) + v(t) \sin(\omega t), \tag{26}$$

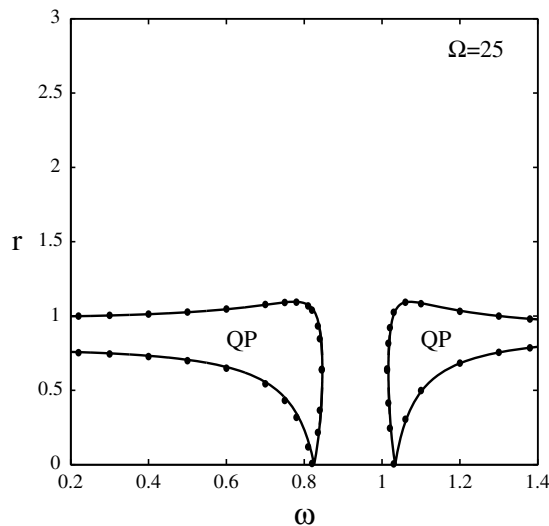


Fig. 2. Modulation amplitude vibration for $\Omega = 25$. Analytical approximation: Solid lines, Numerical simulation: dots. QP: modulation area of QP responses.

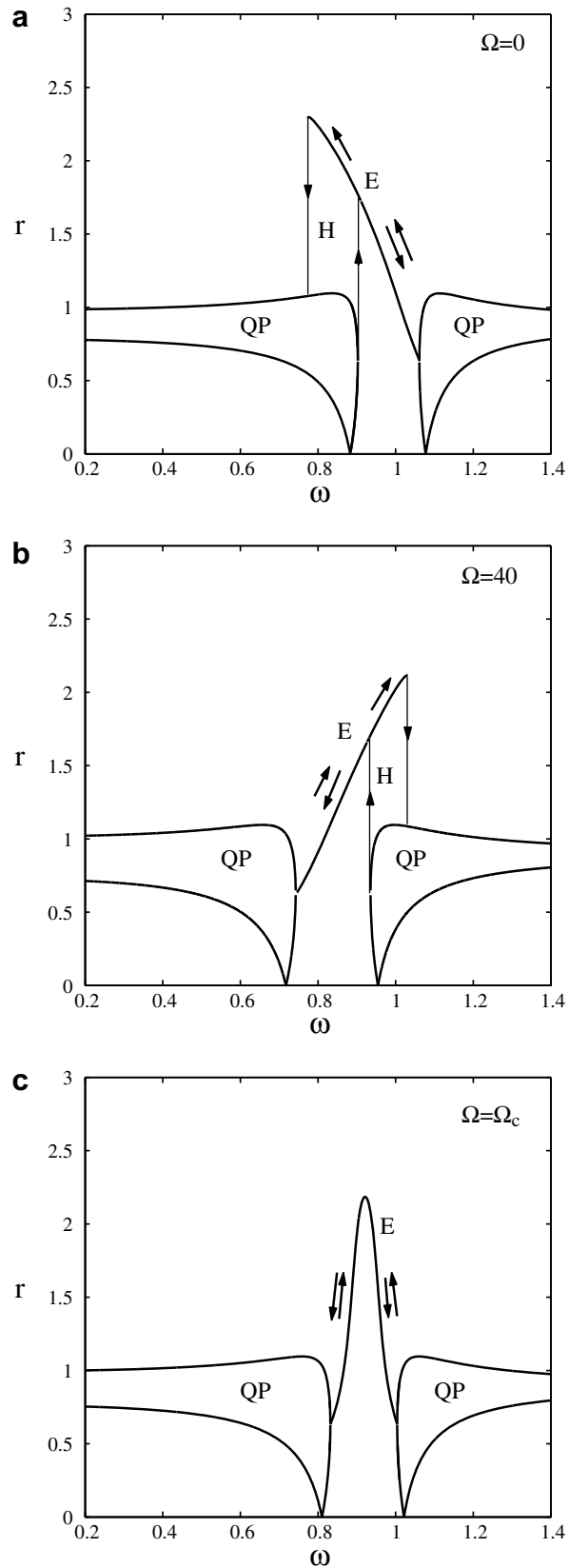


Fig. 3. Effect of the frequency Ω on the hysteresis loop. H: hysteresis loop; E: entrainment area.

where the amplitude R and the phase φ are obtained by setting $\frac{dR}{dt} = 0$ and given respectively by

$$R = \sqrt{\frac{4\alpha}{\beta} - \frac{2h^2}{\sigma^2}}, \tag{27}$$

$$\varphi = -\left(\frac{3\xi\sigma}{8\omega|\sigma|}R^2 + \frac{3\xi h^2}{4\omega\sigma|\sigma|}\right)t. \tag{28}$$

Using (25), the modulated amplitude of QP oscillations is approximated by using the relation

$$r(t) = \sqrt{u^2(t) + v^2(t)} = \sqrt{\frac{4\alpha}{\beta} - \frac{h^2}{\sigma^2} + 2R\frac{h}{\sigma} \cos(vt + \varphi)}. \tag{29}$$

Therefore, the QP modulation area is delimited by the curves given by the two conditions

$$r_{\min} = \min \left\{ \sqrt{\frac{4\alpha}{\beta} - \frac{h^2}{\sigma^2} + 2R\frac{h}{\sigma}}, \sqrt{\frac{4\alpha}{\beta} - \frac{h^2}{\sigma^2} - 2R\frac{h}{\sigma}} \right\}, \tag{30}$$

$$r_{\max} = \max \left\{ \sqrt{\frac{4\alpha}{\beta} - \frac{h^2}{\sigma^2} + 2R\frac{h}{\sigma}}, \sqrt{\frac{4\alpha}{\beta} - \frac{h^2}{\sigma^2} - 2R\frac{h}{\sigma}} \right\}. \tag{31}$$

In Fig. 2 we draw, for $\Omega = 25$, the modulated QP area given by Eqs. (30) and (31) (solid lines) and numerically using Runge–kutta method (dots). The comparison between the results shows a very good agreement and confirms the accuracy of the analytical approach used here. In contrast, the approach used in [14], based on the invariance of the slow flow (16) under the transformation $\theta \rightarrow -\theta + \frac{\pi}{2}$, $\sigma \rightarrow -\sigma$ and $\xi \rightarrow -\xi$ presented a discrepancy between the theory and the simulation, especially in the vicinity of jumps phenomena. Fig. 2 shows that outside the synchronization area, QP behavior with two predominant frequencies takes place. Moving away from the synchronization area, the amplitude depth decreases. When approaching the entrainment area, the lower band of the modulation amplitude domain drops to zero, and then increases to collide with the upper limit of the modulation amplitude, exactly on the loci where the frequency-locked response takes place. Note that this dynamic has not been captured analytically by using the invariance approach [14].

In Fig. 3a and b, we show the global picture of the amplitude–frequency response for the values $\Omega = 0$ and $\Omega = 40$. Fig. 3c illustrates the frequency response for the critical case Ω_c corresponding to the vanishing of the nonlinear characteristic stiffness ξ of the slow dynamic (11). This threshold is given by

$$\Omega_c = \frac{\sqrt{3\gamma}}{a}. \tag{32}$$

By studying the sign of the discriminant Δ given by (18), we obtain an analytical approximation of the hysteresis area as illustrated in Fig. 3a and b. In Fig. 4, we plot this hysteresis area as a function of the excitation frequency Ω . It can be seen from Fig. 4 that a complete elimination of the hysteresis is achieved in a certain range of the frequency Ω delimited approximately by $\Omega \simeq 24.3$ and $\Omega \simeq 30.4$. The threshold $\Omega_c \simeq 27.4$ given by (32) is located exactly in the middle of the suppression

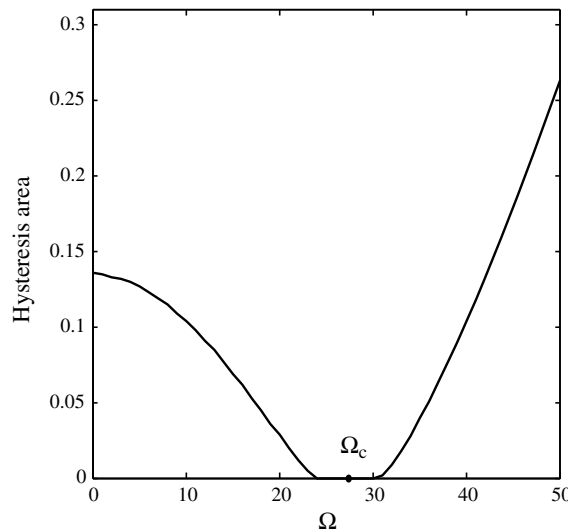


Fig. 4. Variation of the hysteresis area versus the frequency Ω . Analytical result, Eq. (18).

domain (see Fig. 4). In this domain jump phenomenon is completely eliminated and hence a smooth transition between the QP response and the frequency-locked motion takes place. This analytical prediction illustrated in Fig. 4 is confirmed by comparison to numerical simulations provided in Fig. 1.

4. Conclusion

In this paper, we have studied the effect of a FHE on hysteresis in a forced van der Pol–Duffing oscillator near the fundamental resonance 1:1. We have performed an analytical approach based on averaging and multiple scales technique and derived successively a slow dynamic, its slow flow and a slow slow flow. Analysis of equilibria and limit cycle of these flows provides explicit analytical expressions of the entrainment area, the QP modulation domain and the area of the hysteresis. We have shown that a FHE can suppress hysteresis for a certain range of the fast frequency preventing jumps between two stable states and offering a smooth transition between QP response and an entrained motion in the system. Numerical simulation was carried out and confirmed the analytical finding. This result suggests that in the case where damping and non-linearity are fixed in certain applications or in specific experiments, a FHE can be an alternative to effectively eliminate hysteresis in a relatively large range of the fast excitation frequency.

Acknowledgment

The hospitality of LaMcos, INSA-LYON is gratefully acknowledged by author MB.

References

- [1] Pandey M, Rand RH, Zehnder AT. Perturbation analysis of entrainment in a micromechanical limit cycle oscillator. *Commun Nonlinear Sci Numer Simul* 2007;12:1291–301.
- [2] Nayfeh AH, Younis MI, Abdel-Rahman EM. Dynamic pull-in phenomenon in MEMS resonators. *Nonlinear Dyn* 2007;48:153–63.
- [3] Stephenson A. On induced stability. *Philos Mag* 1908;15:233–6.
- [4] Hirsch P. Das pendel mit oszillierendem Aufhängepunkt. *Zeitschrift für Angewandte Mathematik und Mechanik* 1930;10:41–52.
- [5] Kapitza PL. Dynamic stability of a pendulum with an oscillating point of suspension. *Zurnal Eksperimental'noj i Teoreticeskoj Fiziki* 1951;21:588–97 (in Russian).
- [6] Thomsen JJ. Some general effects of strong high-frequency excitation: stiffening, biasing, and smoothing. *J Sound Vib* 2002;253(4):807–31.
- [7] Jensen JS, Tcherniak DM, Thomsen JJ. Stiffening effects of high-frequency excitation: experiments for an axially loaded beam. *J Appl Mech* 2000;67:397–402.
- [8] Hansen MH. Effect of high-frequency excitation on natural frequencies of spinning discs. *J Sound Vib* 2000;234(4):577–89.
- [9] Tcherniak D, Thomsen JJ. Slow effect of fast harmonic excitation for elastic structures. *Nonlinear Dyn* 1998;17:227–46.
- [10] Mann BP, Koplou MA. Symmetry breaking bifurcations of a parametrically excited pendulum. *Nonlinear Dyn* 2006;46:427–37.
- [11] Sah SM, Belhaq M. Effect of vertical high-frequency parametric excitation on self-excited motion in a delayed van der Pol oscillator. *Chaos Solitons Fract* 2008;37(5):1489–96.
- [12] Belhaq M, Sah SM. Horizontal fast excitation in delayed van der Pol oscillator. *Commun Nonlinear Sci Numer Simul* 2008;13(8):1706–13.
- [13] Pandey M, Rand RH, Zehnder AT. Frequency locking in a forced Mathieu–van der Pol–Duffing system. *Nonlinear Dyn* 2007. doi:10.1007/s11071-007-9238-x
- [14] Belhaq M, Fahsi A. 2:1 and 1:1 frequency-locking in fast excited van der Pol–Mathieu–Duffing oscillator. *Nonlinear Dyn* 2007. doi:10.1007/s11071-007-9302-6
- [15] Blekhman II. *Vibrational mechanics – nonlinear dynamic effects, general approach, application*. Singapore: World Scientific; 2000.
- [16] Belhaq M, Houssni M. Quasi-periodic oscillations, chaos and suppression of chaos in a nonlinear oscillator driven by parametric and external excitations. *Nonlinear Dyn* 1999;18:1–24.
- [17] Belhaq M, Guennoun K, Houssni M. Asymptotic solutions for a damped non-linear quasi-periodic Mathieu equation. *Int J Nonlinear Mech* 2002;37:445–60.
- [18] Rand RH, Guennoun K, Belhaq M. 2:2:1 Resonance in the quasi-periodic Mathieu equation. *Nonlinear Dyn* 2003;31:187–93.
- [19] Rand R, Morrison T. 2:1:1 Resonance in the quasi-periodic Mathieu equation. *Nonlinear Dyn* 2005;40:195–203.
- [20] Sah SM, Recktenwald G, Rand RH, Belhaq M. Autoparametric quasiperiodic excitation. *Int J Nonlinear Mech* 2008;43:320–7.
- [21] Nayfeh AH, Mook DT. *Nonlinear oscillations*. New York: Wiley; 1979.